Flame Lengths Under Ceilings

Vytenis Babrauskas
Center for Fire Research, National Bureau of Standards, Washington, DC 20234, USA

The evaluation of hazards from developing room fires often requires a knowledge of flame lengths developed by burning objects. Procedures for estimating flame lengths have been available only for vertical plume fires, where there is no flame impingement on the room ceiling. Calculational procedures are developed for approximate calculation of flame lengths when part of the flame flow is along the ceiling. Four common geometries are treated: unbounded ceiling, plume near corner, plume in corner and one-directional corridor spread. Ceiling flame lengths are calculated by use of the assumption that the total air entrained up to the flame tip is the same for ceiling flow as for the free fire. Comparison with limited experimental data suggests potential for prediction in full-scale room fires.

INTRODUCTION

Room fires often start in a small, discrete object near the floor. A plume, consisting of a burning zone followed beyond the flame tip by hot non-combusting gases, extends upward above this burning object. With increasing burning rate the flames may reach the ceiling. With further increase they will effectively mushroom out and flow along the ceiling, as in Fig. 1. If the room contains additional fuel items, nearby but outside of direct flame contact, these may be ignited from the flame radiant flux. The ignition potential for these items will be related to, among other things, the view angle to the flames. When spread of flames along the ceiling occurs this angle may be significantly increased, compared to the situation, where a ceiling is not present, and the flames merely become slightly taller. This phenomenon has qualitatively been known for a long time, but has not been treated quantitatively in practical cases. It is of interest, therefore, to make some simple calculations and to obtain some approximate answers. Consideration will be limited to burning objects which can be approximated as a horizontal pool, usually, but not necessarily, at floor level. The ultimate fuel is gaseous; it may come from pyrolysis of a liquid or solid fuel or, for experimental purposes, simple gas burners can be used.

FREE FLAME LENGTHS

Flame heights above simple fuel sources burning in the open have long been studied. Blinov and Khudiakov[1, 2] measured flames above circular pans of burning liquids. In the turbulent regime they observed that the flame height h_f varied with pan diameter D as

$$\frac{h_f}{D} \sim 1.7 \tag{1}$$

Thomas *et al.*[3] conducted experiments on wood cribs and showed that from simple scaling considerations one expects that

$$\frac{h_f}{D} \propto \left[\frac{(\rho w)^2}{D^5}\right]^n \tag{2}$$

where ρ and w are the cold fuel density and volume flow rate, respectively. The exponent n varied for different test series and was around 0.3. In a later paper, Thomas[4] analysed additional experiments and established that h_f/D depends on the Froude number, Fr. The Froude number is the ratio of initial momentum to buoyancy and is defined as

$$\mathrm{Fr} = \frac{(\dot{m}_0/A_0)^2}{\rho_a^2\, gD}$$

Here A_0 is the source area $\pi D^2/4$, $\dot{m}_0$ is the fuel mass flow rate, ρ_a is the ambient air density, and $g = 9.81$ m s^{-2}. For Fr than ~ 0.01, $n = 1/5$ and the flame lengths become independent of diameter, giving

$$h_f = 18\, \dot{m}_0^{2/5} \tag{3}$$

Later, Steward[5] analysed further flame height data and provided a theory based on actual solution of conservation equations. Comparison of theory with experiment showed that visible flame tips corresponded to a distance in which five times the stoichiometric combustion air had been entrained. Fang[6] adopted the same model and obtained more detailed solutions. Both their solutions involved a complex but weak dependence on fuel composition. Fang also provided a simpler expression in the form

$$\frac{h_f}{D} = \frac{K}{2^{4/5}} = \mathrm{Fr}^{1/5} \tag{4}$$

Inserting $\rho_a = 1.2$ kg m^{-3} gives

$$h_f = K\,(0.37)\, \dot{m}_0^{2/5} \tag{5}$$

The constant K ranged between 26 and 60 for the data Fang compared, giving

$$h_f = (9.6 \text{ to } 22.2)\, \dot{m}_0^{2/5} \tag{6}$$

This range circumscribes Thomas's constant of 18.

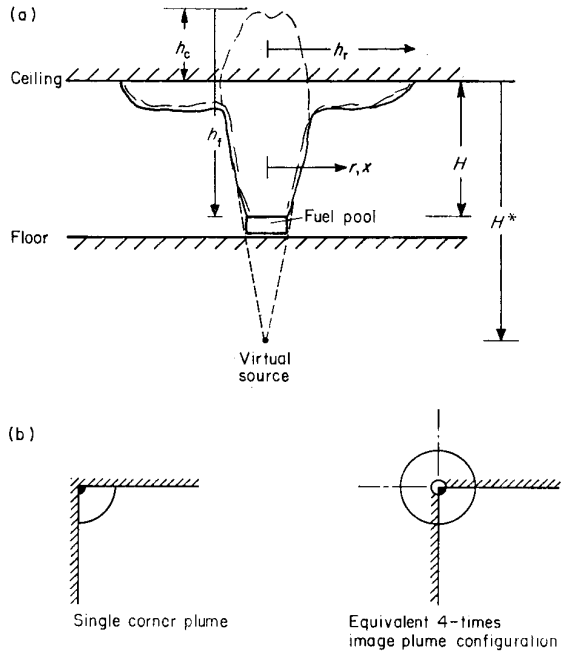

Figure 1. Geometry and flame length nomenclature: (a) basic geometry—vertical section through room; (b) corner configuration—plan view.

The exact fuel-composition dependent formulation for K can also be evaluated. For methane fuel into normal atmosphere $K=49.7$. Since fuel composition effects are small, it will be assumed here that the fuel is similar to methane.

The above expressions can also be evaluated in terms of heat flow units. For methane, using $Q/\dot{m}_0 = 50 \times 10^3$ kW/(kg s^{-1}) and $K=49.7$ gives

$$h_f = 0.24\ Q^{2/5} \tag{7}$$

The most recent flame length measurements have been reported by McCaffrey,[7] burning natural gas, largely methane. He found a continuous flame region that terminates at a height

$$h = 0.08\ Q^{2/5} \tag{8}$$

and an intermittent flaming region that continues up to

$$h = 0.20\ Q^{2/5} \tag{9}$$

Thus, the agreement with the older work is good if the flame tip is considered the end of the intermittent zone. The region beyond the flame tip is termed the free plume.

PLUME ENTRAINMENT AND MASS FLOWS

The model for combustion in the flame zone above the pool is as follows: pure fuel is released at the fuel source at a relatively low velocity. Entrainment of pure air takes place into plume from its sides. Let the ratio of entrainment velocity to centerline axial velocity be k_e. This number is taken to be a constant, approximately 0.1 in plumes far away from the combustion region, but is not necessarily constant in the lower regions. Except very close to the source the total mass flux in the flame or plume is predominantly the entrained fluid, and the source term can be neglected. According to this simple model, the flame tip would correspond to the height at which the stoichiometric air amount had been entrained plus a certain height beyond that, sufficient to cool the products to a temperature where visible radiation would not be seen. In fact, Steward's data[5] show that the tip corresponds to 500% of the stoichiometric air. This is because the air and fuel do not mix and react instantaneously.

Thomas[4] made some crude measurements and, based on dimensional analysis, suggested the flow rate at a given height h is

$$\dot{m} \propto D h^{3/2} \tag{10}$$

This can be compared to the classical expression for plumes, derived from Rouse *et al.*[8] by inserting properties of the standard atmosphere,

$$\dot{m} = 0.056\ Q^{1/3} h^{5/3} \tag{11}$$

where Q is the source heat release rate in kW. The plume expression is applicable only in regions far away from the source.

If the details of combustion are included, the Steward and Fang model can yield an expression where, as shown by McCaffrey and Rockett,[9]

$$\dot{m} \propto h^{5/2}$$

This expression was not borne out by the experimental findings of the same investigation, which showed that near the fuel source

$$\dot{m} \propto \dot{m}_0^{2/3}\ h^{5/6}$$

More recent studies have been made by McCaffrey[7] and Cox and Chitty[10] using laboratory natural gas burners with flow rates of the order 10–100 kW. Their work is significant since detailed measurements were made in the lower portions of the plume. A combined expression, using the functional form devised by McCaffrey, along with a width variation following that of Cox and Chitty yields

$$\dot{m} = C_1 x^2\ Q^{1/5} (h\ Q^{-2/5})^{1-n} \ln [C_2 (h Q^{-2/5})^{2n-1} + 1] \tag{12}$$

where

$$x = 0.106\ Q^{2/5} (0.16 + h Q^{-2/5})$$

$$C_1 = \frac{2\pi g \rho_a C_0^2}{k}$$

$$C_2 = \frac{1}{2g} \left(\frac{k}{C_0}\right)^2$$

$$C_0 = 0.9$$

and in the three regions

continuous flame	$k=6.8$	$n=1/2$
intermittent flame	$k=1.9$	$n=0$
plume	$k=1.1$	$n=-1/3$

The relationship is plotted in Fig. 2. At the flame tip, h_f, the flow is by combining Eqns (9) and (12), simply

$$\dot{m}|_{h_f} = 0.007\ Q \tag{13}$$

For other arbitrary heights there is no simple expression.

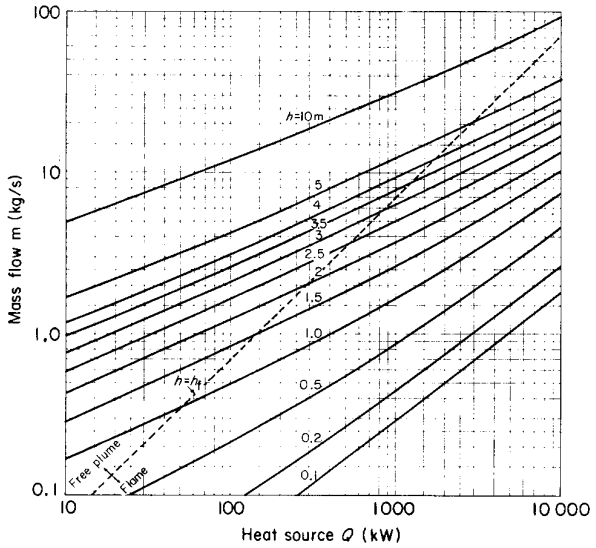

Figure 2. Entrained flow rates in a vertical plume.

CEILING ENTRAINMENT

When a horizontal ceiling is present above the fire, the plume flow turns upon hitting the ceiling and now flows horizontally. Air is still being entrained into the flow stream and comes in at a right angle to the main flow, i.e. vertically upwards. This geometry is sometimes termed a 'ceiling jet'. Compared to the large amount of studies available in vertical plumes, data are extremely scarce on ceiling layer flows. Basically, only two studies are available. Ellison and Turner[11] measured ceiling layer entrainment as a function of the Richardson number, Ri. Their data can be approximated as

$$k_e = 0.12\, e^{-3.9\ \mathrm{Ri}} \tag{14}$$

The Richardson number requires a knowledge of the ceiling flows and is, thus, not available *a priori*. Alpert[12] constructed numerical solutions for a heated, noncombusting axisymmetric plume impinging on an unbounded ceiling. Alpert compared his solutions to a very limited range of experimental data. The range of validity has not been fully explored; however, his results will be used since no other comparable study is available. Using his solutions, an expression for k_e can be obtained as

$$k_e \sim 0.12\,(1 - e^{-0.6/(r/H)}) \tag{15}$$

where r is the radial distance along the ceiling and H is the ceiling height above the pool. Thus, the local entrainment decreases from its plume value with increasing ratios r/H. This entrained air flow along the ceiling can then be obtained by integrating.

$$d\dot{m} = \rho_a k_e v\, dA$$

where v is the characteristic jet flow velocity, and dA, the area through which entrainment takes place, is $2\pi r dr$.

CASE I: UNBOUNDED CEILING, UNRESTRICTED PLUME

This case is important because it is the simplest and an expression for k_e is available. Taking $k_e(r)$ as in Eqn 15 and $dA = 2\pi r dr$; then only $v(r)$ is needed. From Alpert's solutions[12] this can be approximated as

$$v(r) \sim \frac{0.72}{r/H}\left[\frac{Qg}{H\rho_a C T_a}\right]^{1/3} \tag{16}$$

where C is the heat capacity and T_a is the ambient temperature of the gas. To obtain the ceiling flow entrained up to a certain radius r_1, we should integrate $d\dot{m}$ from r_e, the plume radius at the ceiling, up to r_1.

$$\int d\dot{m} = Z \int (1 - e^{-B/r})\, dr \tag{17}$$

where

$$B = 0.6\, H$$

and

$$Z = 0.54\, \rho_a\, H \left[\frac{Qg}{H\rho_a C T_a}\right]^{1/3}$$

evaluating ρ_a, C and T_a, this yields

$$Z = 0.20\, H^{2/3}\, Q^{1/3}$$

The integral can be evaluated numerically or with the use of the tabulated special function E_1. In Fig. 1(a) the ceiling spread distance h_r is defined to be measured from the centerline. A simplified view of the turning region is then taken by assuming that no entrainment takes place along the ceiling within the plume confines of $r < r_e$. Alpert's results show that $r_e/H = 0.17$, therefore the ceiling mass flows are integrated from a starting point of $r = r_e = 0.17\, H$. This integration has been performed and the results are shown in Fig. 3. The flow rate is described non-dimensionally as $\dot{m}/ZB$, or $\dot{m}/(0.12\, H^{5/3} Q^{1/3})$.

Alpert's ceiling flow relationships were developed for the case where the fuel source is far away from the ceiling and the plume flows can be represented as a free plume. Since the interest here is in the near-field case, a correction should be made for the fact that the fuel source area is substantial, not infinitesimal compared to H. This 'virtual source' correction is most simply performed by using Alpert's relationship that r/H scales in the ratio 0.17:1. Thus, a simple approximate correction can be made by replacing the actual height H in Fig. 3 with a virtual height H^*, given by

$$H^* = H + 2.94\, D \tag{18}$$

where D is the burner diameter. This correction should

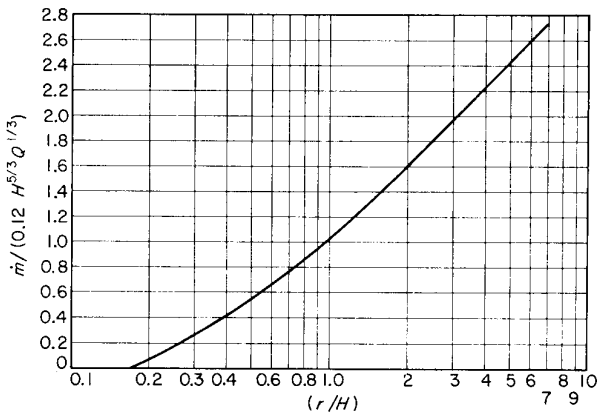

Figure 3. Ceiling flows, axisymmetric case.

not be applied to the plume flows (Fig. 2) since these have been derived from measurements with finite-area burners.

A geometric adjustment of this kind to get the virtual source is, of course, quite crude. A more refined analysis would take into account the fact that plume width near the burner is not necessarily equal to the burner width. One approach would be to use the experimental plume half-widths, x, as determined by Cox and Chitty[10] or McCaffrey[7]. Then a calculated $D \propto Q^n$ would result, where $n=2/5$ or $1/2$, respectively. The D calculated by this procedure would depend only on Q and be entirely independent of actual burner diameter. Thus, it is not clear that such correction is substantially better than the simple one above, especially in view of the non-existence of experimental data covering a range of burner diameters.

Consider now an example appropriate for a full-size room fire. Take $Q=500$ kW, $H=2.0$ m. The fire diameter D will be taken as small compared to H; therefore D does not enter as a variable. Then from Eqn (9) $h_f=0.20(500)^{2/5}=2.40$ m. If the fuel is considered to be methane, the stoichiometric combustion would require 500 $(17.2)/(50\times10^3)=0.17$ kg s^{-1} air. Here 17.2 is the air:fuel ratio and 50×10^3 kJ kg^{-1} is the methane net calorific value. From Fig. 2, at a height of h_f the flow is 3.5 kg s^{-1}, or 21 times the stoichiometric amount. This can be compared to Steward's ratio of 5. The difference arises because of the different values used for entrainment into the plume. Another study, by Becker and Yamazaki,[13] suggests that under the present conditions of fully free convection, $\dot{m}=0.0063\ Q$ at h_f, giving a ratio of 18.5 times stoichiometric in this case. Becker and Yamazaki attribute the increased entrainment to large-scale turbulence.

Since a relationship for visible flame length dependence on mass flow rates has not been directly measured for ceiling flows, the following reasonable, but unproven, assumption will be made. For a given source strength, the same total amount of air must be entrained for ceiling flows as for plume flows. Therefore, in the example, the flame tip in the ceiling would correspond to the point where a total of 3.5 kg s^{-1} air had been entrained. The plume entrainment over the ceiling height H is from Fig. 2, equal to 2.72 kg s^{-1}. The flame tip will then correspond to the distance h_r at which an additional $3.5-2.72=0.78$ kg s^{-1} had been entrained. We assume that $D \ll H$, therefore, $H \sim H^*$. Then from Fig. 3 a flow of 0.78 kg s^{-1} is entrained at $r/H=0.30$, or $h_r=0.60$ m.

The ceiling spread distance h_r is larger than the 'cut-off' height h_c in the ratio $0.60/(2.40-2.0)=1.50$. This ratio is quite sensitive to the flows of Eqns (3) and (7). At the present time, neither of these are known with significant certainty. For example, the flows derived by McCaffrey[7] and Cox[10] differ roughly by a factor of 1.8. If the flows in Eqn (12) are multiplied by 1.8, the resultant h_r/h_c ratio becomes 2.25 in the present example.

Experimental verification

Experimental measurements of h_r and h_c have recently been reported for this geometry by You and Faeth.[14, 15] They used several varieties of fuel but in small scale and at low heat flow rates ($Q<10$ kW). Their data are shown in Table 1. The method of analysis used in the theoretical model is based on mass flows as the primary variable. Consequently, the results can be interpreted more readily if converted to a mass flow basis. A theoretical ceiling $\dot{m}$ value is obtained by using the relationship shown in Fig. 3 for the ceiling flow occurring at the measured r/H. The required ceiling $\dot{m}$ value is obtained as the difference between the $\dot{m}$ at the (measured) h_f and the $\dot{m}$ at H. The relative agreement of these two values indicates the adequacy of theoretical predictions. A plot of this comparison, shown in Fig. 4, shows that disagreement is scale dependent. For the smaller fires Eqn (9) under-predicts ceiling entrained flows quite significantly. The general trend of the data as well as an exponential curve fit suggests that for full-sized room fires ($Q\sim1000$ kW) flows might approach closer agreement. Further experimental work is necessary to clarify this point.

Effects of varying H/h_f

Since neither the plume nor the ceiling layer entrains uniformly with distance, it is likely that the h_r/h_c ratio is a function of H/h_f. To determine this, calculations can be made for a fixed fuel flow but varying H/h_f. The fire Q will again be taken as 500 kW and H varied. The results are shown in Fig. 5. In the range of $0.5<H/h_f<0.85$, h_r is larger than h_c by a ratio of 1.20 to 2.0, reaching the minimum near $H/h_f=0.7$. Note that, as a consequence of the definition adopted for h_r, at $H/h_f=1.0$ and correspondingly $h_c=0$, h_r is equal to 0.17 H and not zero. These relationships are only slightly dependent on the value of Q; thus, the trends in Fig. 5 should hold for most full-scale room fires.

CASE II: FULL PLUME, 1/4 CEILING

Several practical combustion arrangements can be approximated by the following simple idealization. The freely entraining plume, as above, is impinged on a ceiling where only a 90° sector is allowed for gas flow. This might occur, say, if the fire is close to a room corner, but not so close that the plume 'attaches' to the corner. The entrainment into the plume would then be essentially unchanged. In the ceiling layer, however, the flow area would be reduced by a factor of 4. A direct theoretical analysis is not available for this case. However, the ceiling flows are similar† to those that would result from a fire of four times the strength, flowing into 360° of ceiling. The plume itself, however, is assumed far enough from the corner so that no change in flows results.

For a 500 kW fire below a 2.0 m ceiling, the needed ceiling flow is still $3.5-2.72=0.78$ kg s^{-1}. For the ceiling flow, however, $\dot{m}=4(0.78)\times3.12$ kg s^{-1} and $Q=4(500)=2000$ kW are taken. From Fig. 3, $r/H=0.60$ and $h_r=1.20$ m. This yields an h_r/h_c ratio of 3.0, which is substantially greater than the 1.50 ratio for an unbounded ceiling.

† This assumption, while seemingly straightforward, is somewhat of a simplification. Experimental observations of room-sized ceiling jets do not show fractional axisymmetric patterns when placed in a corner or against a wall. Instead, a channeling effect is observed, with increased flows and temperatures near the walls.

Table 1. Ceiling flame lengths, You and Faeth data

Q (kW)	Measured h_f (m)	$\dot{m}$ at h_f (kg s^{-1})	H (m)	Virtual H^* (m)	$\dot{m}$ at H (kg s^{-1})	Required ceiling flow $\dot{m}$ (kg s^{-1}) (1)	Measured h_r (m)	r/H^*	Theo ceiling flow $\dot{m}$ from r/H^* (kg s^{-1}) (2)	Ratio (1)/(2)
Methanol										
0.366	0.138	0.0027	0.076	0.179	0.00122	0.0015	0.035	0.20	0.0003	5.1
0.620	0.204	0.0057	0.076	0.226	0.00161	0.0041	0.051	0.23	0.0011	3.67
0.620	0.204	0.0057	0.127	0.227	0.00303	0.0027	0.038	0.14	—	—
1.19	0.304	0.0130	0.076	0.299	0.00229	0.0107	0.095	0.32	0.0049	2.17
1.19	0.304	0.0130	0.127	0.350	0.0042	0.0126	0.066	0.19	—	—
1.19	0.304	0.0130	0.260	0.483	0.0106	0.0024	0.026	0.05	—	—
2.26	0.350	0.0212	0.076	0.391	0.0033	0.0179	0.120	0.31	0.0086	2.09
2.26	0.350	0.0212	0.206	0.521	0.0106	0.0106	0.089	0.17	—	—
Ethanol										
0.410	0.152	0.0032	0.076	0.179	0.00129	0.0019	0.046	0.26	0.0009	2.03
0.707	0.229	0.0070	0.076	0.226	0.0017	0.0053	0.060	0.27	0.0018	2.88
1.54	0.356	0.0180	0.076	0.299	0.00265	0.0154	0.101	0.34	0.0064	2.44
1.54	0.356	0.0180	0.127	0.350	0.0048	0.0132	0.082	0.23	0.0031	1.53
1.54	0.356	0.0180	0.260	0.483	0.0120	0.0060	0.028	0.06	—	—
1.54	0.356	0.0180	0.336	0.559	0.0167	0.0013	0.006	0.01	—	—
2.77	0.444	0.032	0.076	0.391	0.0037	0.0283	0.155	0.40	0.0145	1.96
2.77	0.444	0.032	0.206	0.521	0.0117	0.0203	0.146	0.28	0.0131	1.56
Propanol										
0.360	0.170	0.0034	0.076	0.179	0.00121	0.0022	0.057	0.32	0.0015	1.51
0.360	0.170	0.0034	0.127	0.230	0.00237	0.0010	0.041	0.18	—	—
0.786	0.254	0.0084	0.076	0.226	0.00183	0.0066	0.070	0.31	0.0028	2.36
0.786	0.254	0.0084	0.127	0.277	0.0034	0.0050	0.060	0.22	0.0014	3.65
1.64	0.394	0.0212	0.127	0.350	0.0049	0.0163	0.101	0.29	0.0059	2.76
1.64	0.394	0.0212	0.260	0.483	0.0124	0.0088	0.052	0.11	—	—
1.64	0.394	0.0212	0.336	0.559	0.0173	0.0039	0.032	0.06	—	—
3.29	0.521	0.0426	0.076	0.391	0.0042	0.0384	0.190	0.49	0.0203	1.91
3.29	0.521	0.0426	0.206	0.521	0.0127	0.0299	0.152	0.29	0.0138	2.16
Pentane										
0.778	0.254	0.0084	0.076	0.179	0.00181	0.0066	0.081	0.45	0.0030	2.20
0.778	0.254	0.0084	0.127	0.230	0.00338	0.0050	0.077	0.33	0.0030	1.64
1.62	0.356	0.0185	0.076	0.226	0.0027	0.0158	0.092	0.41	0.0051	3.11
3.46	0.508	0.042	0.076	0.299	0.0043	0.0377	0.190	0.64	0.0170	2.22
3.46	0.508	0.042	0.127	0.350	0.0074	0.0346	0.187	0.53	0.0189	1.83
3.46	0.508	0.042	0.260	0.483	0.0176	0.0244	0.124	0.26	0.0108	2.26
3.46	0.508	0.042	0.336	0.559	0.0025	0.0395	0.098	0.18	—	—
7.89	0.686	0.093	0.076	0.391	0.0073	0.0857	0.356	0.91	0.0474	1.81
7.89	0.686	0.093	0.206	0.521	0.0200	0.0730	0.292	0.57	0.0500	1.46

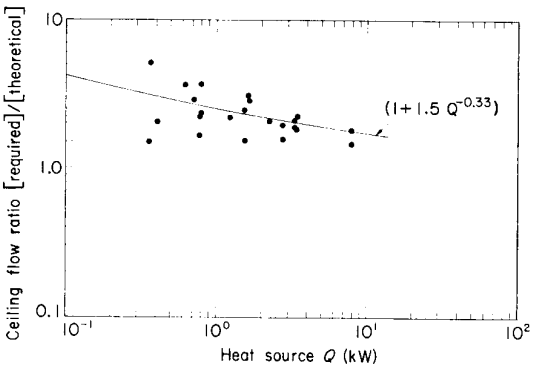

Figure 4. Small-scale data by You and Faeth on ceiling flows.

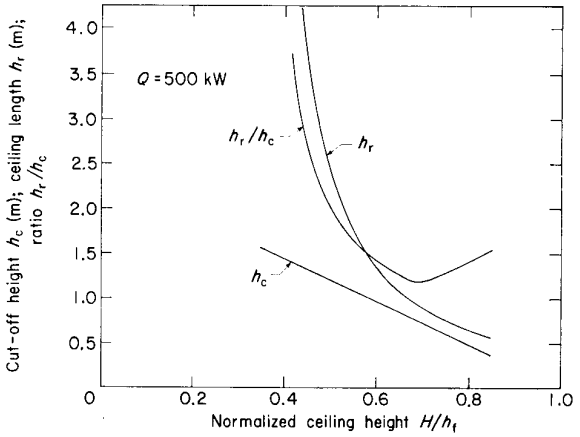

Figure 5. Theoretical flame lengths for unbounded ceilings.

CASE III: 1/4 PLUME, 1/4 CEILING

If a fire is placed close to the corner the radial air entrainment will be changed. If it is close enough, the flame will 'attach' to the walls. In that case there is no more entrainment, except from the open direction. The ceiling flow will again only fill a 90° sector. This case can be solved simply by using the method of images for the whole flow [Fig. 1(b)]. The flame lengths are calculated as in Case 1, except that an effective Q of four times the actual one is used for both plume and ceiling flows. The only additional error introduced by this kind of analysis is a very slight one due to the neglect of viscous effects at the walls.

Using the Case I example, a 500 kW fire will be placed in the corner, making an effective $Q=2000$ kW. The same height $H=2.0$ m is assumed. Figure 2 indicates $\dot{m}=14.0$ kg s^{-1} at h_f and 5.42 kg s^{-1} at the ceiling, leaving a flow of 8.58 kg s^{-1} to be entrained in the (effective full) ceiling flow. From Fig. 3 the r/H is 2.4, giving $h_r=4.8$ and $h_r/h_c=12$.

CASE IV: CORRIDOR SPREAD

The final case of considerable interest is one where a freely entraining plume impinges on a corridor ceiling; the flow then goes lengthwise in one direction only. No theoretical analysis is available for this case. The closest characterized model is one from an earlier study by Alpert.[16] In that study Alpert considered an infinite line plume impinging on a ceiling and flowing equally in both directions. This can be easily converted to a single direction flow by considering an equivalent plume across an image plane, yielding an effective fire size twice as large as actual. Alpert's numerical solutions show that the approximate functional form for k_e is the same as for the axisymmetric case. If the requirement is enforced that $k_e=0.12$ at $x=0$, then exactly the same expression as before results:

$$k_e=0.12\,(1-e^{-0.6/(x/H)}) \tag{19}$$

Here x is the distance along the ceiling flow, instead of r. Similarly the results for ceiling flow velocity can be expressed as

$$v\sim\frac{1.2}{(x/H)^{1/5}}\left(\frac{Qg}{b\rho_a C T_a}\right)^{1/3} \tag{20}$$

where b is the corridor width. Note that this expression differs from the one for the axisymmetric case in that both H and b are needed, and in the small power dependence on x. If the plume we are trying to model is circular, rather than a line source, an additional discrepancy is introduced. This error will probably be small, however, since it only involves plume shape effects far from the point of interest in the ceiling layer.

To get mass flows, we integrate

$$d\dot{m}=\rho_a\,k_e\,v\,b\,(2dx)$$

to obtain

$$\dot{m}=0.11\,HQ^{1/3}b^{2/3}\int^{x_1/H}\left(\frac{H}{x}\right)^{1/5}(1-e^{-0.6(H/x)})\,d(x/H) \tag{21}$$

The lower limit for integration can again be taken as

Table 2. Corridor flame lengths

Q (kW)	H (m)	Virtual H^* (m)	Theo $\dot{m}$ at flame tip (kg s^{-1})	Theo $\dot{m}$ at H (kg s^{-1})	Required ceiling flow $\dot{m}$ (kg s^{-1}) (1)	b (m)	Observed h_r (m)	x/H^*	Theo ceiling flow $\dot{m}$ from x/H^* (kg s^{-1}) (2)	Ratio (1)/(2)
Hinkley										
600	1.20	3.10	4.20	1.57	2.63	1.2	5.0	1.61	2.86	0.92
	0.90	2.80	4.20	1.13	3.07	1.2	6.5	2.32	3.34	0.92
	0.66	2.56	4.20	0.82	3.38	1.2	6.9	2.70	2.95	1.15
500	1.20	3.10	3.50	1.43	2.07	1.2	4.0	1.29	2.40	0.86
	0.90	2.80	3.50	1.03	2.47	1.2	4.5	1.61	2.43	1.02
	0.66	2.56	3.50	0.74	2.76	1.2	4.7	1.84	2.10	1.31
360	1.20	3.10	2.52	1.20	1.32	1.2	2.5	0.81	1.62	0.82
	0.90	2.80	2.52	0.86	1.66	1.2	4.0	1.43	2.05	0.81
	0.66	2.56	2.52	0.61	1.91	1.2	3.6	1.41	1.85	1.03
246	1.20	3.10	1.72	0.99	0.73	1.2	1.5	0.48	0.89	0.82
	0.90	2.80	1.72	0.70	1.02	1.2	3.0	1.07	1.55	0.66
	0.66	2.56	1.72	0.49	1.23	1.2	2.0	0.78	1.14	1.08
	0.37	2.27	1.72	0.27	1.45	1.2	3.0	1.32	1.40	1.03
168	1.20	3.10	1.18	0.83	0.35	1.2	0	—	—	—
	0.90	2.80	1.18	0.57	0.61	1.2	1.0	0.36	0.48	1.27
	0.66	2.56	1.18	0.40	0.78	1.2	0.75	0.29	0.31	2.54
	0.37	2.27	1.18	0.21	0.97	1.2	1.3	0.57	0.68	1.42
Atallah										
56	0.34	1.34	0.39	0.10	0.29	0.36	2.47	1.84	0.27	1.08
42	0.34	1.34	0.29	0.09	0.20	0.36	1.52	1.13	0.19	1.06
28	0.34	1.34	0.20	0.07	0.13	0.36	0.81	0.60	0.10	1.25
									Average	1.11

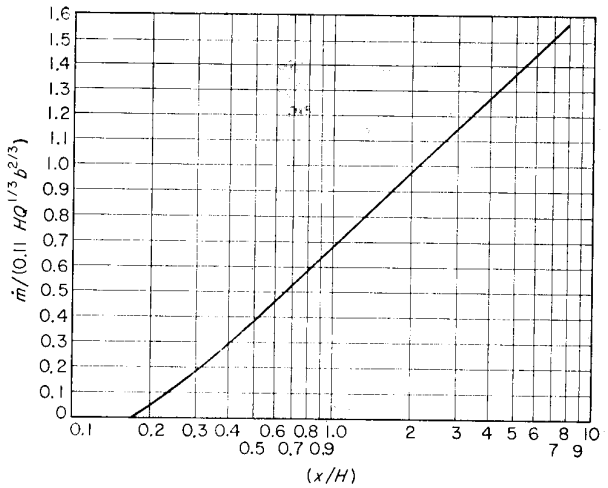

Figure 6. Ceiling flows, 2-dimensional case.

0.17. The expression was integrated numerically. Results are given in Fig. 6.

Consider now a specific example. Let the fire $Q = 500$ kW and $H = 2.0$ m be discharging one way down the corridor ceiling. Then the effective $Q = 1000$ kW. At the ceiling this will give a flow of 3.79 kg s^{-1} while at $h_f =$ 3.17 m the total flow is 7.0 kg s^{-1}. The cut-off height h_c is 1.17 m. Assume a reasonable corridor width $b = 3$ m. Then from Fig. 6 flames will extend to the point where an additional 3.21 kg s^{-1} flow is picked up, or $x/H = 1.06$, giving $h_r = 2.12$ m. The h_r/h_c ratio is 1.81. This result is strongly dependent on corridor width. If the width is 2 m, the h_r/h_c ratio rises to 2.94.

Experiments in corridors

Two series of similar experiments have been reported where flame lengths were measured along a corridor ceiling. Atallah[17] and Hinkley *et al.*[18] used porous gas burners impinging flames onto a ceiling with single direction flow. Atallah also conducted additional experiments with burners in the ceiling, but these will not be considered here. The analysis will have to be very crude since rectangular burners were used in a configuration resembling neither symmetric area sources nor line sources. We will consider these to be equivalent to a wall-scale (1/2 plume) geometry and apply an effective doubling rule. Thus, if Q is actually released by the burner, for plume entrainment we will assume that the $\dot{m}$ of 1/2 is that from a $2Q$ fire.

The calculations are shown in Table 2. A virtual source correction was made using Eqn (10) in the same manner as for axisymmetric flows. The agreement between flows deduced from measured flame lengths and flows computed from Eqn (12) is quite good, the theoretical values being on the average 10% too low. Over the whole range of experimental heat rates (28 to 600 kW) there is no systematic deviation.

CONCLUSIONS

Simple calculational procedures have been developed to allow the prediction of ceiling flame lengths for a plume near a corner, plume in a corner, and one-directional corridor spread. The application is limited to a simple fuel geometry and noncombustible room surfaces. The procedures were based on the limited theoretical models and sketchy available data. Experimental results tend to corroborate the predicted trends to an adequate degree for full-scale room fires (Q around 100–1000 kW); for small fires ($Q \sim 1$ kW) overly long flame lengths are predicted.

Several experimental areas are seen as needing investigation. Plume measurements over a wider range of flows and burner sizes are needed. A more refined procedure for virtual source correction could yield improved overall accuracy. Ceiling layer mass flows should be carefully examined. The criterion for defining the ceiling flame tip needs to be carefully examined. Here it was taken as being the point where the same amount of air had been entrained as at the tip of the free flame. This criterion may not be valid if ceiling mixing rates are substantially different or boundary heat loss effects are significant. The actual ceiling jet flow patterns should be studied for 90° and 180° jet geometries. Finally, full-scale experiments in the same geometries as considered here would enable a better assessment of the calculational procedures, or result in improved procedures.

Acknowledgements

The development of the concepts in this paper was aided materially by discussions with Bernard McCaffrey and John Rockett.

REFERENCES

1. V. I. Blinov and G. N. Khudiakov, *Diffusion Burning of Liquids,* US Army Corps of Engineers Translation T-1490 a-c. Moscow (1961).
2. V. I. Blinov and G. N. Khudiakov, Certain laws governing diffusive burning of liquids. *Fire Res. Abstr. Rev.* **1**, 41 (1958).
3. P. H. Thomas, C. T. Webster and M. M. Raftery, Some experiments on buoyant diffusion flames. *Combust. and Flame* **5**, 359 (December 1961).
4. P. H. Thomas, The size of flames from natural fires, in *Ninth Symposium (International) on Combustion* pp. 844–859 (1963).
5. F. R. Steward, Prediction of the height of turbulent diffusion buoyant flames. *Combust. Sci. Technol.* **2**, 203 (1970).
6. J. B. Fang, Analysis of the behavior of a freely burning fire in a quiescent atmosphere. NBSIR 73-115, National Bureau of Standards, Washington DC (1973).
7. B. J. McCaffrey, Purely buoyant diffusion flames: some experimental results. NBSIR 79-1910. National Bureau of Standards, Washington, DC (1979).
8. H. Rouse, C. S. Yih and H. W. Humphreys, Gravitational convection from a boundary source. *Tellus* **4**, 201 (1952).
9. B. J. McCaffrey and J. A. Rockett, Static Pressure Measurements of Enclosure Fires. *J. Res. Nat. Bur. Stand.* **82**, 107 (1977).
10. G. Cox and R. Chitty, A study of the deterministic properties of unbounded fire plumes, unpublished.
11. T. H. Ellison, J. S. Turner, Turbulent entrainment in stratified flows. *J. Fluid Mech.* **6**, 423 (1959).
12. R. L. Alpert, Turbulent ceiling-jet induced by large-scale fires. Report 22357–2. Factory Mutual Research Corp., Norwood, Mass. (1974).

13. H. A. Becker and S. Yamazaki, Entrainment, momentum, flux and temperature in vertical free turbulent diffusion flames. *Combust. Flame*, **33**, 123 (1978).
14 H. Z. You and G. M. Faeth, *An Investigation of FireImpingement on a Horizontal Ceiling,* Mechanical Engineering Dept., Pennsylvania State University, University Park (1978).
15. H. Z. You and G. M. Faeth, Ceiling heat transfer during fire plume and fire impingement. *Fire Mat*, **3**, 140–147. (1979).
16 R. L. Alpert, Fire induced turbulent ceiling-jet. Report 19722–2. Factory Mutual Research Corp., Norwood, Mass. (1971).
17 S. Atallah, Fires in a model corridor with a simulated combustible ceiling, Part I—radiation, temperature and emissivity measurements. (Fire Research Note 628). Fire Station, Borehamwood (1966).
18 P. L. Hinkley, H. G. H. Wraight and C. R. Theobald, The contribution of flames under ceilings to Fire spread in compartments, Part I incombustible ceilings. Fire Research Note 712. Fire Research Station, Borehamwood (1968).

Received 8 October 1979

APPENDIX: NOMENCLATURE

A	area (m^2)
A_0	area of fuel pool (m^2)
b	corridor width (m)
C	heat capacity (kJ kg^{-1} K^{-1})
D	diameter of fuel pool (m)
Fr	Froude number
g	acceleration of gravity (m s^{-2})
H	pool to ceiling distance (m)
H^*	virtual source to ceiling distance (m)
h	height (m)
h_c	cut-off (free minus ceiling) height (m)
h_f	flame length in free plume (m)
h_r	flame radial extent along ceiling (m)
k	constant in Eqn (12)
k_e	entrainment constant
$\dot{m}$	mass flow rate (kg s^{-1})
$\dot{m}_0$	fuel flow rate (kg s^{-1})
n	constant in Eqn (12)
Q	fuel heat release rate (kW)
r	radial distance (m)
r_e	plume radius at junction with ceiling jet (m)
Ri	Richardson number
T_a	ambient temperature (K)
v	characteristic ceiling jet velocity (m s^{-1})
w	fuel volume flow rate (m^3 s^{-1})
x	plume half-width (m); distance along ceiling jet in 2-dimensional case (m)
ρ	fuel gas density (kg m^{-3})
ρ_a	ambient air density (kg m^{-3})